Pattern Recognition in Photoacoustic Dataset

R. Guzmán-Cabrera, J. R. Guzmán-Sepúlveda, M. Torres-Cisneros, D. A. May-Arrioja, J. Ruiz-Pinales, O. G. Ibarra-Manzano, et al.

International Journal of Thermophysics
Journal of Thermophysical Properties and Thermophysics and Its Applications

ISSN 0195-928X

Int J Thermophys
DOI 10.1007/s10765-013-1452-9

Int J Thermophys
DOI 10.1007/s10765-013-1452-9

Pattern Recognition in Photoacoustic Dataset

R. Guzmán-Cabrera · J. R. Guzmán-Sepúlveda · M. Torres-Cisneros · D. A. May-Arrioja · J. Ruiz-Pinales · O. G. Ibarra-Manzano · G. Aviña-Cervantes

Received: 16 February 2012 / Accepted: 3 May 2013

Abstract In photoacoustic imaging, optical absorption properties of matter are imaged by detecting the ultrasound that is produced when the material is illuminated by a laser. For medical imaging, photoacoustics is a useful tool since matter in the human body has different optical absorption properties. In this study, pattern recognition systems are used to study a set of medical images for tumor identification and extraction—to detect the specific area in which the tumor is present. The objective is to incorporate this information into real-time image acquisition systems to improve medical diagnosis. Preliminary results obtained by studying the image dataset demonstrated the interchangeability of the proposed system. A system of automatic classification was constructed, using a set of images with and without cancerous tumors to evaluate the proposed method. The training set used was manually labeled, and the test set was never seen by the training set. The results helped us determine the feasibility of the proposed system.

Keywords Pattern recognition · Photoacoustic · Tumor

R. Guzmán-Cabrera (✉) · M. Torres-Cisneros · J. Ruiz-Pinales · O. G. Ibarra-Manzano · G. Aviña-Cervantes
División de Ingenierías del campus Irapuato—Salamanca,
Carretera Salamanca—Valle de Santiago km 3.5+1.8 km Comunidad de Palo Blanco,
36885 Salamanca, GTO, México
e-mail: guzmanc@ugto.mx

J. R. Guzmán-Sepúlveda · D. A. May-Arrioja
Unidad Académica Multidisciplinaria Reynosa—Rodhe, Universidad Autónoma de Tamaulipas,
Carretera Reynosa—San Fernando cruce con canal Rodhe, Colonia Arco iris,
88779 Reynosa, TAMPS, México

Published online: 24 May 2013

1 Introduction

In the recent years, it has been demonstrated that computer-aided diagnosis systems are effective tools in diagnostic support, since they are capable of providing radiologists and internists with a reliable second opinion that can be used even in the first stage of patient examination. For this purpose, the development of suitable tools and techniques is required to detect and recognize abnormal features in the human body and then to analyze, discriminate, and extract them. Photoacoustic imaging is a relatively new hybrid imaging modality that combines both light–matter interaction and ultrasound imaging [1] providing detailed information about the physiology of the tissue in a graphical manner. In doing so, optical technique advantages, such as high contrast and spectroscopic-based specificity, and high spatial resolution of ultrasound, can be provided by this hybrid imaging method. The photoacoustic technique involves targeting nanosecond pulses of visible laser light to the surface of the skin, and the absorption of the laser energy results in rapid thermoelastic expansion and the emission of broadband pulses of ultrasound, typically on the order of tens of MHz. The latter propagates to the surface where they are detected at different spatial points using either an array of ultrasound receivers or a single mechanically scanned detector.

By measuring the arrival time of the ultrasound pulses on the surface and knowing the speed of sound in the tissue, an image of the absorbed optical energy distribution can be reconstructed. Spatial resolution is defined by the physics of ultrasound propagation and is limited by the frequency-dependent attenuation characteristics of soft tissue. Image contrast is strongly dependent on optical absorption, which makes this technique particularly suitable for blood vessel imaging because of the strong optical absorption properties of hemoglobin. Other studies have shown that by using photoacoustic methods, changes in tissue perfusion, which is characteristic of skin tumors [2], as well as dermal vascular lesions and soft tissue damage, such as burns [3], can be observed. The virtue of being noninvasive and the capability of imaging without harmful side effects are the main advantages of photoacoustic techniques. As a result, photoacoustic imaging has been extensively studied, and notable results have been published for imaging in humans and small animals [4–6]. In order to perform quality photoacoustic imaging, the acoustic transducer should be able to provide good axial and lateral resolution, high sensitivity, wide bandwidth, and should ideally acquire a complete three-dimensional (3D) image with a single shot at fast frame rates, without scanning [7]. These requirements are partially contradictory (i.e., resolution and sensitivity) or are limited by current technology (3D acquisition and transparency to laser pulse).

Photoacoustic tomography is a natural complement to existing ultrasonography and should enlarge the scope of ultrasound in diagnostic imaging and therapeutic monitoring of various types of cancer (e.g., prostate cancer), by providing additional information. Previous studies have demonstrated that the growth of new blood vessels, known as angiogenesis, is an inherent element of metastasis in most solid tumors, including prostate and breast cancers. Owing to the high sensitivity of blood, photoacoustic tomography may be a useful tool in evaluating physiological characteristics of the tissue, such as tumor-related vascular distortion, including both angiogenesis and dilation of blood vessels in cancerous tissues, in a conclusive way to provide reliable support to medical diagnosis [8]. The increase of blood volume in tumor regions, a typical functional hallmark of prostate cancer, might be reliably detected and localized by photoacoustic tomography with high optical contrast and high spatial resolution.

Despite the advantages of photoacoustic imaging, there are still some challenges to achieve better performance. For instance, in the so-called backward mode detection configuration, an array of transparent optical detectors placed on the skin are required to adequately measure the excitation laser pulses transmitted through it and into the underlying tissue. This presents obvious difficulties when using piezoelectric transducers, because they are typically opaque—a notable exception has been described in [9]. Another challenge arises because most image reconstruction algorithms require the detector element size to be small when compared with the acoustic wavelength. For surface-imaging applications, where the acoustic propagation distances are just a few millimeters, the signal is only weakly band-limited by frequency-dependent acoustic attenuation. This results in broadband signals (tens of MHz) with wavelengths as small as a few tens of microns. Achieving adequate detection sensitivity with elemental sizes on this scale becomes problematic because of the inverse relationship between the active area of a piezoelectric actuator and its sensitivity. All previous challenges are currently being tackled, but significant changes in the existing technology are required. For this reason, systems for computational image processing, such as the one proposed in this study, have been chosen to overcome hardware limitations.

In this study, a set of medical images is analyzed, using pattern recognition techniques that help in detecting the area where the tumor is localized. The objective is to incorporate this information into real-time systems for image acquisition to improve medical diagnosis. Results will help us determine the feasibility of the proposed method.

2 Method

Being capable of finding abnormalities (i.e., tumors, abnormal blood flow, and temperature changes) in photoacoustic images is an activity that requires experts, and considering that it is necessary to efficiently complement the medical diagnosis using machine learning techniques, the development of new tools is imperative. This is the central idea of this study, i.e., to offer an alternative technique in identifying and discriminating suspicious areas based on the extraction features through texture analysis. Since texture-based analysis methods characterize texture in terms of the extracted features, segmentation depends not only on the images under study but also on the purpose for which the image texture analysis is used.

As stated before, the proposed technique is based on texture segmentation, which is performed by using entropy analysis. In this particular case, the local entropy for a small region Ω_k by a window size $(M_k \times N_k)$ within the input image, which has been drawn as the first stage of the proposed algorithm, is defined as follows [10,11]:

$$E(\Omega_k) = -\sum_{i=0}^{L-1} P_i \log(P_i) \tag{1}$$

where

$$P_i = \frac{n_i}{M_k \times N_k} \tag{2}$$

is the probability of grayscale i appearing in the neighborhood Ω_k and n_i is the number of pixels with grayscale i in the neighborhood. L is the maximal grayscale, and $E(\Omega_k)$ is the local entropy of the neighborhood Ω_k. A texture image is then generated using entropy filtering, and then a rough mask of the bottom texture (i.e., background) is created. The background mask, which is used as a contrast mask along with the original image, allows identifying and then extracting the regions of interest (i.e., top textures). In other words, the implemented system takes a photoacoustic image as input, which is first used to create a texture image, and is then used to create a rough mask for the bottom texture. Next, the rough mask is used to segment the top texture, and finally, the segmentation result is displayed. The information displayed is potentially useful to strengthen medical diagnosis. The test and results of the described method are presented in the next section.

3 Test and Results

To demonstrate the advantages of the proposed system for visualizing potential tumors, tests have been performed on several images. All images were obtained using noninvasive techniques, without signal averaging, and using an incident beam with power levels below the maximum permissible limit for safe exposure of the skin.

3.1 Test 1: Noncancerous Mass

Figure 1 shows the photoacoustic image of a human palm showing its vasculature. The image dataset is available online for viewing and downloading as animated volume-rendered images and movie files at stacks: iop.org/PMB/54/1035 [12] or the University College London Website [13]. These animations provide the most compelling demonstrations of the 3D-imaging capability of the system.

Figure 2 is a snapshot of a graphical user interface showing the same image being tested. In this case, a noncancerous mass is present in the image. As can be noticed, several processes are simultaneously performed on the image being studied: primitive enhancement by normalizing the image (i.e., histogram stretching), segmentation and extraction of the identified structures, and pseudocoloring with three different color maps (i.e., thermal, spectral, and parametric dynamic pseudocoloring [14]). It should be emphasized that this study focuses on the segmentation and extraction processes, while enhancement and pseudocoloring are only used to support the obtained results.

Segmentation and extraction techniques are based on the feature extraction through texture analysis for identifying and discriminating suspicious areas mainly related to cancer and benign tumors. Texture and morphologic differences in the abnormality region allows it to be identified and then analyzed, to discriminate, and extract it, and hence, the first stage in the proposed algorithm consists in recovering the structural

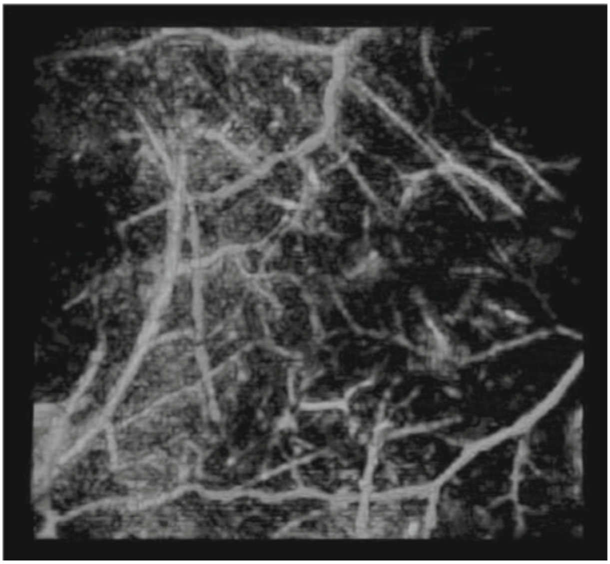

Fig. 1 *In vivo* photoacoustic image of the vasculature in the palm using an excitation wavelength of 670 nm

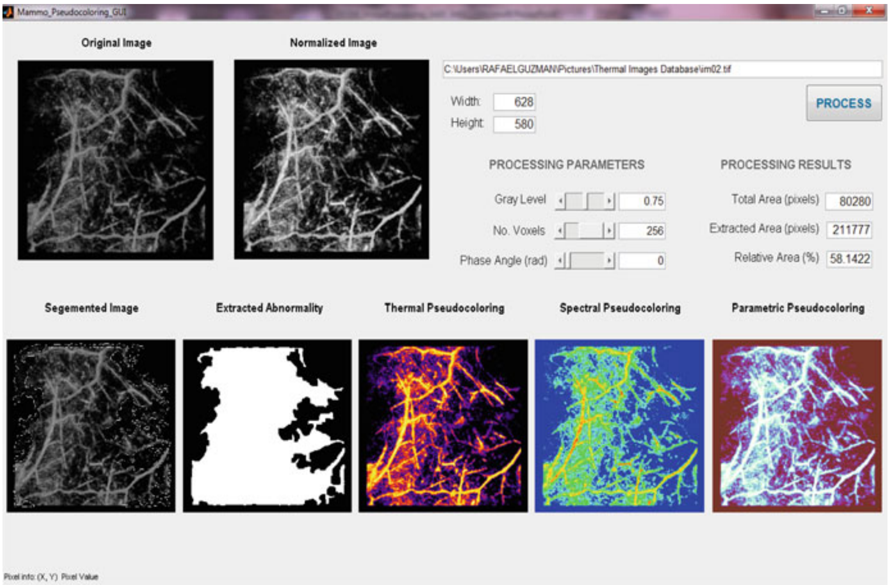

Fig. 2 Graphical interface of the implemented system to find abnormalities in photoacoustic images

information of the original image through the local entropy with a standard 9×9 window. Once the structural information is represented in the image resulting from the entropy filtering, a threshold is performed on this first texture image to get a binary texture image. An additional cleaning of the overly segmented binary image is

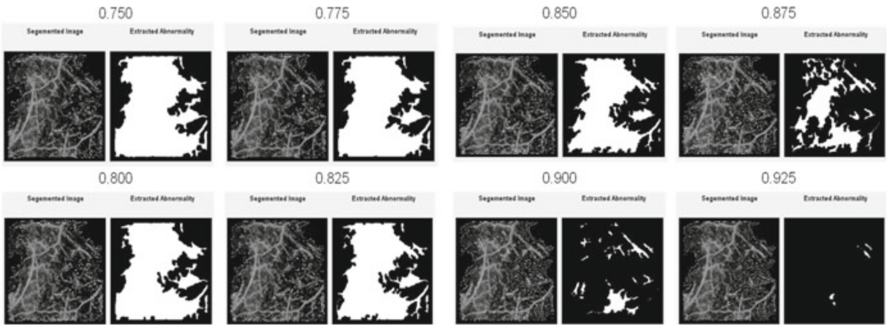

Fig. 3 Segmentation (*left* of each sub-image) and extraction (*right* of each sub-image) for different reference *gray levels*

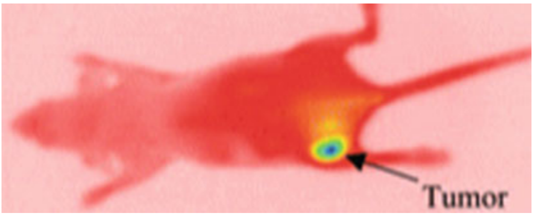

Fig. 4 Mouse model with implanted subcutaneous tumor

performed to remove all the "small" regions that are not significant in the segmentation process. The segmented regions from the binary texture are then filled, their edges are smoothed, and then by using the generated rough mask, it is possible to extract the texture of interest.

When the image is processed with the implemented algorithm, it can be observed that different layers are separated depending on the reference gray level. In this particular case, the threshold value to obtain the binary texture is the relative gray level of the pixels in the abnormality region and, since the gray level represents the intensity detected by the sensor, this reference value is directly related to the depth of the layer thus allowing for direct correlation between the identified texture in the tissue and its depth (Fig. 3).

3.2 Test 2: Cancerous Mass

Small animals (i.e., mice models) are used to study the pathophysiology of a wide variety of tumors to support the development and refinement of new cancer therapies. As shown in Fig. 4, the most common approach is to implant a subcutaneous tumor and to study its progression over time. Characterizing the structure of the tumor vasculature is important as it can affect the development of the tumor and its response to treatment.

In a similar way to the example shown in the previous section, segmentation and extraction are performed on the image. As shown in Fig. 5, the result is the successful extraction of the tumor region with a different extent depending on the reference gray-level value in which the processing is performed.

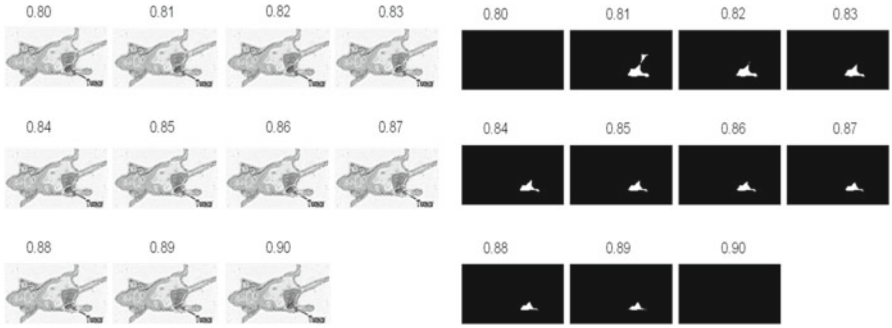

Fig. 5 Segmentation (*left*) and extraction (*right*) on the image of a tumor-implanted mouse

In terms of the reference gray level, the obtained results showed that this value strongly determines the area that is identified and then extracted. It can be clearly noticed that as the reference gray value increases, the amount of extracted area decreases and additionally, a cleaner extraction of the hand-marked area is achieved.

Results show that for lower values of the reference gray level, most of the abnormality is identified and extracted, but some other regions with similar textures also appear. For larger values of the reference gray level, regions with similar textures gradually disappear from the image, but the abnormality region is still identified and discriminated with a smaller area.

According to the obtained results, an adequate value of the reference gray level allows one to achieve a successful segmentation and extraction of the suspicious regions, while they are discriminated in a clear and effective way, avoiding, as much as possible, the extraction of nonrelevant regions with similar textures. In terms of medical diagnostic support, the capability to discriminate suspicious from nonrelevant regions could be a difficult task because important information related to possible abnormal regions can be omitted. Therefore, the method that has been developed in this study provides a very simple way to overcome the problems without compromising crucial information that could avoid the detection of potential tumors.

4 Conclusions

cA method for pattern recognition is proposed for tumor identification and extraction from a set of thermoacoustic images. The proposed algorithm has the potential of being incorporated into real-time systems for image acquisition to improve medical diagnosis.

The training set that was used was manually labeled, and the test set was never seen by the training set. The main parameter to control the performance of the proposed algorithm is the reference gray level around which the abnormality will be searched. The obtained results suggest that, supplemented with an adequate value of the reference gray level, the proposed method provides the capability to achieve a successful segmentation and extraction of the suspicious regions, while they are discriminated in a clear and effective way, avoiding the extraction of nonrelevant regions with similar textures as much as possible.

Since the reference gray level of the proposed method can be easily adjusted, it provides a simple and versatile way to discriminate suspicious regions from nonrelevant regions without compromising crucial information that could avoid the detection of potential tumors. The tests results of the extraction of carcinogenic masses in photoacoustic images allow validating the effectiveness and suitability of the proposed method since the obtained information can complement the medical diagnosis providing additional information for better decision making.

References

1. M. Xu, L. Wang, Rev. Sci. Instrum. **77**, 041101 (2006)
2. J.T. Oh, M.L. Li, H.F. Zhang, K. Maslov, G. Stoica, L.V. Wang, J. Biomed. Opt. **11**, 34032 (2006)
3. J.G. Laufer, D.T. Delpy, C.E. Elwell, P.C. Beard, Phys. Med. Biol. **52**, 141 (2007)
4. L. Wang, J. Dis. Mark. **19**, 123 (2004)
5. C.G.A. Hoelen, F.F.M. de Mul, R. Pongers, A. Dekker, Opt. Lett. **23**, 648 (1998)
6. J.J. Niederhauser, M. Jaeger, R. Lemor, P. Weber, M. Frenz, IEEE Trans. Med. Imaging **24**, 436 (2004)
7. J.J. Niederhauser, M. Jaeger, M. Frenz, Appl. Phys. Lett. **85**, 846 (2004)
8. G. Ku, X. Wang, X. Xie, G. Stoica, L.V. Wang, Appl. Opt. **44**, 770 (2005)
9. E. Zhang, J. Laufer, P. Beard, Appl. Opt. **47**, 561 (2008)
10. R.C. Gonzalez, R.E. Woods, S.L. Eddins, *Digital Image Processing Using MATLAB*, chap. 11 (Prentice Hall, Upper Saddle River, NJ, 2003)
11. C. Yan, N. Sang, T. Zhang, Pattern Recognit. Lett. **24**, 2935 (2003)
12. E.Z. Zhang, J.G. Laufer, R.B. Pedley, P.C. Beard, Phys. Med. Biol. **54**, 1035 (2009)
13. http://www.medphys.ucl.ac.uk/research/mle/index.htm. Accessed Oct 2011
14. T.M. Lehmanna, A. Kaserb, R. Repgesa, Image Vision Comput. **15**, 251 (1997)